

AIAA 80-1042R

Excitation of the Wall Region by Sound in Fully Developed Channel Flow

K. M. M. Alshamani*

University of Technology, Baghdad, Iraq

and

J. L. Livesey† and F. J. Edwards‡

University of Salford, U. K.

Artificial excitation of wall region flow is attempted using air as the working fluid. Sound is injected into the flow by means of a brass diaphragm mounted flush with the channel wall. When operating, the diaphragm is vibrated at its center, with its rim fixed. The effect of such excitation on the axial turbulence intensity near the wall is examined. Sinusoidal and random excitations are considered. Sinusoidal disturbances corresponding to the inner layer bursting frequency are found to have a negligible effect on the turbulence intensity. Random disturbances can lead to either an increase or a decrease in the turbulence intensity, depending on the particular type of disturbance. The amount of increase or decrease becomes more pronounced as the level of the disturbance increases or the Reynolds number decreases. Furthermore, the influence of the disturbance becomes stronger as the wall is approached.

Nomenclature

a	= diaphragm diameter
d	= half the channel gap
e	= strain gage bridge output voltage
f_0	= frequency of the sinusoidal disturbance, Hz
f	= characteristic inner layer frequency, Hz
I_x	= axial turbulence intensity = $(\bar{u}/U) \times 100$
P_0	= a point with $x/d = 106.5$, $z/d = 5$, $y^+ = 47.2$
r	= axial distance measured from diaphragm center
Re	= Reynolds number = $U_m d / \nu$
RS, SD	= random and sinusoidal disturbance, respectively
T	= inner layer period
$u(t)$	= turbulent velocity fluctuation
\bar{u}	= root mean square value of u
U	= local time mean velocity
U_m	= fully developed value of U at $Y = d$
U_τ	= shear velocity
vib-dia	= vibrator-diaphragm system
W1	= upstream hot wire
W2	= downstream hot wire
x	= axial coordinate measured from channel inlet
y	= distance measured normal to wall (in this study, the bottom wall)
Y	= distance measured normal to the top channel wall
y^+, Y^+	= yU_τ/ν , YU_τ/ν
z	= transverse coordinate (normal to x and y)
Δ	= diaphragm displacement for steady deflections
λ	= percentage increase in I_x
ν	= kinematic viscosity
ω	= circular frequency
ω^+	= $\omega\nu/U_\tau^2$

Introduction

THE flow near a solid boundary has received considerable attention recently. Studies of this region have covered experimental and theoretical investigations. The experimental

work has included visualization tests as well as quantitative measurements.

Kline et al.¹ performed extensive visual and quantitative studies of the inner layer ($y^+ < 40$) in turbulent smooth boundary-layer flows with zero, favorable, and adverse pressure gradients. They found that the inner layer consisted of a repeated three-dimensional pattern of stretched filaments which moved more slowly than the surrounding fluid. These were referred to as "low-velocity" streaks. Within the region $y^+ < 10$, a low-velocity streak would lift gradually away from the wall. When the streak reached the region $y^+ = 8-12$, it would begin to oscillate. The oscillation amplified as the streak moved outward and terminated in a very rapid breakup into eddies. Most of the breakups appeared to occur in the region $10 < y^+ < 30$. After breakup, the streak became contorted and stretched, and a portion of it migrated outward through the boundary layer, usually following identifiable trajectories. In a later study by Kim et al.² the term burst was introduced to cover the lift process of the streak, the oscillatory growth motion, and the breakup. The average time between bursts T was given as

$$T = 0.0001023 / U_\tau^2 \quad (1)$$

This gives a nondimensional frequency ω^+ as

$$\omega^+ = \omega\nu/U_\tau^2 = 2\pi\nu/TU_\tau^2 = 0.06 \text{ approx} \quad (2)$$

where ω is the circular frequency.

Corino and Brodkey³ obtained complementary results to those described above by using visualization methods in the pipe flow. They found that the average ejection frequency of low-speed fluid from the wall region was proportional to U_τ^2/ν . This is in agreement with the flow visualization studies of Achia and Thompson⁴ who found that the period of the wall layer flow disturbance was proportional to U_τ^{-2} for water flow in a pipe.

Einstein and Li⁵ measured the autocorrelation function of the wall pressure fluctuation in the boundary layer of an open flume in which oil was flowing. The autocorrelogram was found to exhibit a periodic component with a period of 0.4 s. They concluded that wall pressure fluctuations consisted of two parts: one due to the turbulence outside the viscous sublayer, which has a random character; and the other, periodic in character, interpreted as being connected with the

Presented as Paper 80-1042 at the AIAA 6th Aeroacoustics Conference, Hartford, Conn., June 4-6 1980; submitted July 18, 1980; revision received June 29, 1981. Copyright © American Institute of Aeronautics and Astronautics, Inc., 1980. All rights reserved.

*Senior Lecturer, Department of Mechanical Engineering.

†Professor of Fluid Mechanics, Dept. of Aeronautical and Mechanical Engineering. Member AIAA.

‡Senior Lecturer, Dept. of Aeronautical and Mechanical Engineering.

periodic generation and disintegration of the sublayer. The kinematic viscosity of the oil used was $6.7 \times 10^{-5} \text{ m}^2/\text{s}$, and the friction velocity was 0.13 m/s . This gives

$$\omega^+ = 0.062 \quad (3)$$

This is in good agreement with the results of Morrison⁶ who found that the most energetic component of the sublayer centered on

$$\omega^+ = 0.07 \quad (4)$$

for $y^+ < 5$ and a wide range of Reynolds numbers.

Rao et al.⁷ carried out an experimental study of the turbulent boundary layer using air as the working fluid. They found that the mean time between bursts T , when scaled with the inner variables U_τ and ν , was dependent on Reynolds number. They found

$$T^+ = U_\tau^2 T / \nu = 0.65 Re_\theta^{0.73} \quad (5)$$

where Re_θ is the Reynolds number based on the freestream velocity U_∞ and momentum thickness θ . The range of Re_θ covered was 600-9000. However, when T was scaled with the outer variables U_∞ and δ^* (δ^* is the displacement thickness), Rao et al. found

$$(U_\infty T / \delta^*) = 32 \text{ approx} \quad (6)$$

i.e., a constant independent of the Reynolds number. The independence of T of the Reynolds number when scaling T with the outer variables is further supported by the data of Ueda and Hinze⁸ for boundary-layer flow, giving

$$(U_\infty T / \delta) = 4.7 \quad (7)$$

for $y^+ < 6$, where δ is the boundary-layer thickness. When expressed in terms of U_τ and ν , Eq. (7) gives⁸

$$\omega^+ = 0.027 \quad (8)$$

at $Re_\delta = 35,500$ (Re_δ is the Reynolds number based on U_∞ and δ).

On the other hand, Meek⁹ examined the various measurements of the mean sublayer period and concluded that the mean period scaled with the inner variables U_τ and ν rather than the outer variables. He obtained

$$\sqrt{T/\nu} U = 18 \text{ approx} \quad (9)$$

for Reynolds numbers greater than 10^4 . This was based on twice the boundary-layer thickness and bulk velocity. Equation (9) gives

$$\omega^+ = 0.0194 \quad (10)$$

Later work by Blackwelder and Kaplan¹⁰ for boundary-layer flow showed that the average bursting cycle frequency f was approximately given by

$$(U_\infty / f \delta) = (T U_\infty / \delta) = 10 \quad (11)$$

Returning now to the theoretical investigations on the sublayer flow, Einstein and Li^{5,11} formulated a mathematical model which visualized the region near the wall as a thin layer bounded on one side by the turbulent flow and on the other side by the wall boundary. This thin region is characterized by a sudden disintegration followed by a gradual viscous buildup. The period of the sublayer buildup T was given as¹¹

$$T = 172 \nu / U_\tau^2 \quad (12)$$

which gives

$$\omega^+ = 0.0365 \quad (13)$$

Black¹² proposed a similar model giving the frequency of sublayer breakdown as

$$\omega^+ = 0.056 \quad (14)$$

Inner Layer Excitation

It may be argued that there exists a characteristic frequency associated with the inner layer, although there is considerable disagreement between the various investigators on the values of this frequency and how it should be scaled.

If a sinusoidal disturbance having a frequency given by the inner layer frequency is applied to the inner layer, then the inner layer may be excited by this frequency. The present work examines the effect of such a disturbance. Two important points, however, are borne in mind. First, the frequency of the inner layer bursts varies over a certain band, i.e., the time between the bursts is not constant but varies over some average value. Hence one may need to apply a disturbance containing a band of frequencies to which the inner layer may respond. Second, the phase relationship between the applied disturbance and the intermittent motions of the inner layer is important. These effects are examined in the present investigation.

Disturbances are fed into the flow through a circular diaphragm mounted flush with the inner surface of the top wall of a two-dimensional channel built for this purpose. Two types of disturbances are considered: a) a sinusoidal disturbance (SD), and b) a disturbance containing a range of frequencies. Type b is referred to as a random disturbance (RD). The effect of these disturbances is measured in terms of λ , the percentage increase in the axial turbulence intensity resulting from the disturbance.

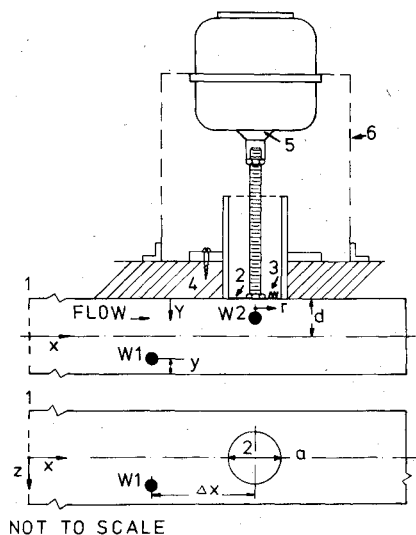


Fig. 1 The vibrator-diaphragm system: 1) channel inlet, 2) diaphragm, 3) strain gages, 4) channel top wall, 5) vibrator, 6) vibrator support, $\Delta x = 13.6 \text{ cm}$, $y_{W1} = 0.156 \text{ cm}$, $z_{W1} = 12.7 \text{ cm}$.

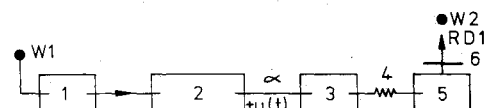


Fig. 2 Feed systems III and IV: 1) DISA anemometer type 55A01; 2) DISA signal indicator and correlator, type 55A06; 3) amplifier; 4) a resistance of 7.5Ω ; 5) vibrator; 6) diaphragm; W1) upstream hot wire; W2) downstream hot wire.

Interaction of Disturbances with the Flow

The interaction of disturbances with the flow may be represented by

$$f(t) + (\text{dia}) + [u(t)]_Q \quad (\text{System I}) \quad (15)$$

where $f(t)$ refers to the applied disturbance, dia to the diaphragm, and $[u(t)]_Q$ to the axial turbulence fluctuation at Q , a typical flow point in the neighborhood of the diaphragm where the effect of $f(t)$ is measured. The disturbance $f(t)$ is either sinusoidal $[f(t)]_{SD}$ or random $[f(t)]_{RD}$. For the former type, we have

$$[f(t)]_{SD} + (\text{dia}) + [u(t)]_Q \quad (\text{System II}) \quad (16)$$

The random disturbances are of two types, referred to as RD1 and RD2. In order to feed RD1 into the flow, the arrangement adopted is to use two hot wires, one upstream and the other downstream of the diaphragm, with a large separation between the wires. These hot wires are referred to as W1 and W2, respectively (Fig. 1). The u fluctuation from W1 is amplified (amp) and fed into the flow through the vibrator-diaphragm (vib-dia) system as a disturbance. In this case we have (Fig. 2)

$$\{\text{amp}[u(t)]_P\}_{RD1} + (\text{dia}) + [u(t)]_Q \quad (\text{System III}) \quad (17)$$

where P refers to the position of W1. The change that occurs in the axial turbulence intensity at Q as a result of feeding RD1 is measured by means of W2 and is expressed in terms of λ which is defined as

$$\lambda = 100 \times [(I_x)_D - (I_x)] / I_x$$

where I_x is the axial turbulence intensity with no disturbance applied, and $(I_x)_D$ the corresponding value with the disturbance.

The effect of inverting the sign of the disturbance is also considered. Thus we have

$$\{\text{amp}[-u(t)]_P\}_{RD1} + (\text{dia}) + [u(t)]_Q \quad (\text{System IV}) \quad (18)$$

Inversion of $u(t)$ was obtained by selecting the appropriate input and output on the correlator. By fixing W1 at a certain point, W2 is moved in the Y direction (Fig. 1) so that the variation of λ with Y may be obtained.

In order to feed RD2, W1 is removed, and only W2 is left in position close to the diaphragm at Q . The output of W2 at Q is fed into the flow as a disturbance by means of the vib-dia system (Fig. 3). By considering a number of points such as Q at the same x and z locations but different Y , the variation of λ with Y may be obtained. Systems IV and III [Interactions (18) and (17)] become, respectively

$$\{\text{amp}[-u(t)]_Q\}_{RD2} + (\text{dia}) + u(t)_Q \quad (\text{System V}) \quad (19)$$

$$\{\text{amp}[u(t)]_Q\}_{RD2} + (\text{dia}) + u(t)_Q \quad (\text{System VI}) \quad (20)$$

Experimental Work

Measurements were made in the fully developed region of a rectangular channel (cross section 5.08×45.72 cm, 335.28 cm long) using air. The air was drawn through the channel by a fan located at the downstream end of the channel. The entrance to the channel consisted of a bell mouth which was enclosed in a large filter box. The axial coordinate x was measured from the channel inlet.

The working section of the channel was provided with Perspex side walls to allow visual observations in the working section. The upper and lower walls of the channel were made of blockboard which was lined with Formica sheets.

The diaphragm was circular in shape, having a diameter a of 3.81 cm and a thickness of 0.038 cm. It was made of brass

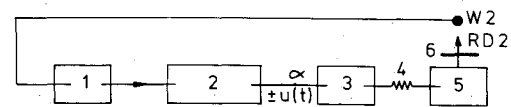


Fig. 3 Feed systems V and VI (legend as in Fig. 2).

and mounted flush with the upper wall of the channel, with its center at $x/d = 111.86$. The diaphragm was soldered to a brass tube. This tube was fixed to the upper wall of the channel (Fig. 1).

The diaphragm was connected at its center to a 7 W Ling Dynamic vibrator, type 101, which had an impedance of 3Ω and a useful frequency range of 1.5-12,000 Hz. The diaphragm was vibrated at its center with its rim fixed.

Four strain gages were attached to the outside surface of the diaphragm. These were arranged in a Wheatstone bridge, and the supply voltage was provided from a Rankintel transistor power pack. The bridge output voltage was read on the DISA rms meter, type 55 D35, and is denoted by e .

The vibrator was driven by a 25 W Derritron power amplifier. This was supplied with a built-in oscillator by means of which sinusoidal disturbances were introduced into the diaphragm (System II). Alternatively, it was possible to feed external random disturbances to this amplifier via an external input, to be subsequently fed after amplification to the diaphragm. In this case, a $12 \mu\text{F}$ capacitor was inserted at the amplifier external input to insure that any dc component contained in the external disturbance might be blocked off, thus avoiding damage to the vibrator. Feed systems III and IV for RD1 are shown in Fig. 2. Feedback systems V and VI for RD2 are presented in Fig. 3.

The relationship between e (volts) and the actual displacement at the diaphragm center Δ (mm) for steady deflections was found from a dial gage calibration of $\Delta = 127e$. Generation of a displacement to the diaphragm occurs only when the vibrator is in operation.

The mean velocity was measured using a total head tube and wall static pressure tapings. The total head tube consisted of a stainless steel tube, having a bore of 0.033 cm and a chamfered working end. This tube was attached to a traversing mechanism that was provided with a Mercer dial gage to indicate the position of the total head tube. This gage was calibrated in 0.01 mm divisions.

Measurement of I_x was made using W2 which was DISA boundary-layer probe (type 55 F 04) in conjunction with DISA hot-wire anemometry. This probe is used for turbulence measurements near a solid boundary. It is gold plated and has prongs parallel to the mean flow direction.

To determine the distance between this wire and the diaphragm, the channel was run at a given Reynolds number and the wire, prior to operation, was traversed gradually toward the wall until the tips of the prongs just touched the surface of the diaphragm. The tips then coincided with their images on the polished surface of the diaphragm. The wire was attached to the prongs so that it was then at a distance of $5 \mu\text{m}$ from the diaphragm. The hot wire was then traversed away from the wall and was fixed at $Y/d = 0.005$. The wire was then operated and turbulence measurements were conducted at this point. Sinusoidal or random excitations were then applied to the diaphragm and turbulence measurements were taken at $Y/d = 0.005$. This allows the calculation of λ at this point. The probe was then traversed to other points in the region $Y/d > 0.005$, where the values of λ were obtained in the same manner. The distance between the upstream hot wire W1 from the shiny white Formica surface was measured using a similar procedure.

The hot-wire probes W1 and W2 were calibrated in the fully developed section of the channel. The calibration is described in two stages. In the first stage, the velocity at the centerline of the channel was measured, using the total head tube, for a

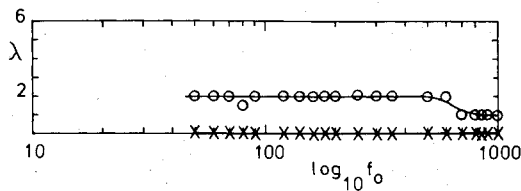


Fig. 4 Variation of λ with external frequency ($Re = 1.52 \times 10^4$, $r/a = z/a = 0$, $e = 2 \times 10^{-4}$ V). ($\circ - Y^+ = 3.8$, $x - Y^+ = 26.7$.)

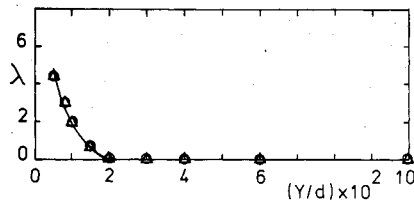


Fig. 5 Profile of λ at $r/a=0$ with feed systems III and IV ($Re = 1.52 \times 10^4$, $e = 3 \times 10^{-4}$ V, W1 is at P_0 , W2 is at $r/a = z/a = 0$). ($\circ - \text{III}$, $\Delta - \text{IV}$.)

number of different flow rates, which were indicated by an orifice meter placed at the downstream end of the fan.¹³ The total head tube was then replaced by the hot-wire probe. The dc voltage E was read from the digital voltmeter (type 55D30) for each previously chosen flow rate. From this a graph of E^2 vs \sqrt{U} was found to be linear, in agreement with King's law.

In the second stage, the total head probe was first positioned at the channel centerline. The flow rate was fixed so that the Reynolds number was $Re = 1.52 \times 10^4$. The total head tube was then traversed toward the wall and the velocity at a certain number of points close to the wall was determined. Then, keeping the Reynolds number at 1.52×10^4 , the total head tube was replaced by the hot-wire probe which was traversed toward the same wall. The dc voltage E was read at the same points at which the velocity had been measured previously. A plot of E^2 vs \sqrt{U} in the second stage was found to give the same linear relationship obtained in the first stage. Accordingly, King's law was found to be very satisfactorily confirmed in present measurements.

Regular checks of the calibration were made in case of a drift resulting from the accumulation of dust particles on the wire. Effective cleaning of the wire was carried out by immersing it in a beaker containing trichloroethylene for about 20 min, and then agitating the liquid acoustically by means of a loud speaker at a frequency of about 50 Hz.

Results

Undisturbed Flow Results

The first stage of the work consisted of obtaining measurements of mean velocity and axial turbulence intensity corresponding to undisturbed flow conditions. Measurements were made of mean velocity and turbulence profiles at various points along the length of the channel. These measurements showed that the flow was two-dimensional over about 90% of its span and that the mean velocity and turbulence profiles were unchanged beyond $x/d = 102$ ($d = 2.54$ cm, half of the channel gap). This is consistent with the study made by Clark¹⁴ who obtained fully developed flow at $x/d = 103$.

Fully developed velocity data in the region $0.012 \leq y/d \leq 1$ and for a wide range of Reynolds numbers gave the law of the wall and velocity defect law, respectively, as¹⁵

$$U^+ = 2.4 \ln y^+ + 3.6$$

and

$$(U_m - U)/U_\tau = -2.7 \ln(y/d)$$

These equations are in general agreement with previously published data on fully developed channel flow.

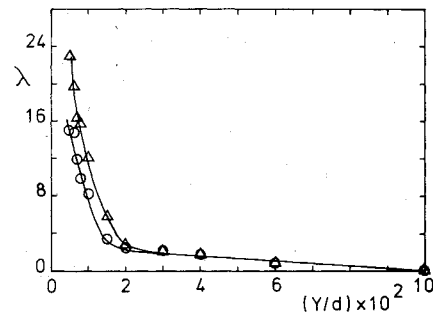


Fig. 6 Profiles of λ at $r/a=0$ with feedback system V ($Re = 1.52 \times 10^4$, W1 removed, W2 at $r/a = z/a = 0$). ($\circ - e = 2 \times 10^{-4}$ V, $\Delta - e = 3 \times 10^{-4}$ V.)

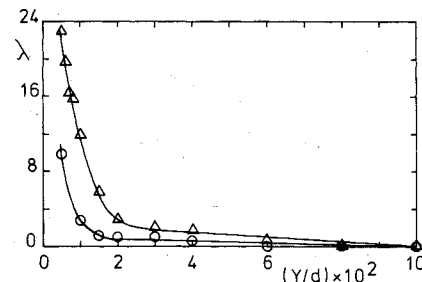


Fig. 7 Profiles of λ at $r/a=0$ with feedback system V ($e = 3 \times 10^{-4}$ V, W1 removed, W2 at $r/a = z/a = 0$). ($\Delta - Re = 1.52 \times 10^4$, $\circ - Re = 6.16 \times 10^4$.)

In addition, the variation of the fully developed values of I_x with y/d was examined for Reynolds numbers ranging from 1.52×10^4 to 6.16×10^4 . Good agreement with previous data was obtained.¹⁵

Sinusoidal Disturbances (System II)

The effect of sinusoidal disturbances is examined here at $Re = 1.52 \times 10^4$ (Fig. 4). At this Reynolds number, the shear velocity U_τ is obtained as 0.45 m/s. To get an estimate of the value of the inner layer frequency, Eqs. (4) and (10) are used. These equations yield high and low values of λ , respectively. For $U_\tau = 0.45$ m/s, the respective values of the inner layer frequency are found to be 150.5 and 41.7 Hz.

To investigate the possibility of finding an external frequency that excites the inner layer bursts, a hot wire was positioned at $r = z = 0$, $Y/d = 0.005$ ($Y^+ = 3.8$), see Fig. 7. Sinusoidal disturbances with frequencies f_0 in the range 20-1000 Hz were fed into the flow via a diaphragm. The disturbance frequency was increased very slowly to identify the critical frequency to which the inner layer might respond in a particularly favorable manner. A similar experiment was repeated at $r = z = 0$, $Y/d = 0.035$, ($Y^+ = 26.7$). (Only a sample of the experimental data are shown in Fig. 4.)

Figure 4 shows that a very small increase in I_x (1-2%) is found at $Y^+ = 3.8$, and no change at $Y^+ = 26.7$. The value of e was kept constant at 2×10^{-4} V for the whole frequency range and for both values of Y^+ . As the hot wire will sense the acoustic waves in addition to the turbulence fluctuations, it is probable that the small increase observed at $Y^+ = 3.8$ is partly due to the hot wire sensing the acoustic waves. Since the values of λ at $Y^+ = 3.8$ are found to be small, in the 1-2% range, no physical significance can be attached to the sudden shift in the values of λ at $f_0 = 600$ Hz. It is also evident from Fig. 4 that no frequency which excites the inner layer bursts is observed.

Random Disturbances, Type 1 (Systems III and IV)

It may be argued that the time between the inner layer bursts is not constant but varies over some average value.

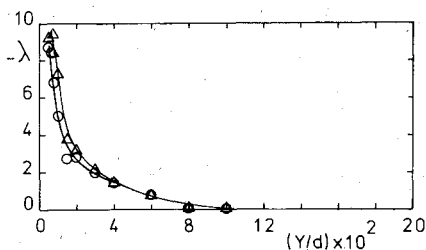


Fig. 8 Profiles of λ at $r/a=0$ with feedback system VI ($Re = 1.52 \times 10^4$, W1 removed, W2 at $r/a=z/a=0$). (\circ — $e = 2 \times 10^{-4}$ V, Δ — $e = 3 \times 10^{-4}$ V.)

Thus a disturbance containing a range of frequencies corresponding to the range of times between the bursts may excite these bursts. Consequently, a disturbance covering the range of 20–20,000 cycles/s was applied to the diaphragm, as such a disturbance would contain the required range of burst frequencies.

Two hot wires are used in this case. The upstream wire W1 is situated at a point with $x/d=106.5$, $z/d=5$, $y^+=47.2$, $y=0.156$ cm (see Fig. 1). This point is referred to as P_0 . With W1 at the edge of the inner layer ($y^+=47.2$), $[u(t)]_{P_0}$ will have a frequency spectrum that may excite the inner layer near the diaphragm.

The downstream wire W2 is positioned at $r=z=0$, $x/d=111.86$, and varying values of Y . The separation between W1 and W2 in the x and z directions is indicated in Fig. 1. With this arrangement, feed system III was employed and the effect on λ in the region $0.005 \leq Y/d \leq 0.1$ was examined.

The results are presented in Fig. 5. The percentage increase in I_x at $Y/d=0.005$ is found to be about 4.5. The value of λ then decreases gradually to zero at $Y/d \geq 0.02$. The profile of λ obtained with system IV is found to be identical to that obtained with system III for the same values of e and Re . This is to be expected, since both of the disturbances $\{\text{amp}[u(t)]_{P_0}\}$ and $\{\text{amp}[-u(t)]_{P_0}\}$ have the same spectral composition, and they are both expected to have zero correlation with the u turbulence fluctuations at flow points near the diaphragm. This is due to the large separation between W1 and W2.

It is conjectured that the small increase in λ is attributed to two factors: 1) W2 senses acoustic waves in addition to turbulence fluctuations; and 2) a change in the turbulence itself may occur as a result of the interaction between the sound field and the turbulence.

Furthermore, it is thought unlikely that this increase in λ is due to the excitation of the inner layer bursts. Under conditions of bursting excitation, λ would be expected to vary according to whether the disturbance $\{\text{amp}[u(t)]_{P_0}\}$ or $\{\text{amp}[-u(t)]_{P_0}\}$ is fed into the flow.

Random Disturbances, Type 2 (Systems V and VI)

The phase relationship between the input disturbance and the bursting events is bound to be an important factor if the flow near the wall is to be significantly affected by the disturbance. Feedback systems V and VI attempt taking the effect of phase into consideration.

Figure 6 shows the effect of feedback system V (employing only W2). λ is plotted against Y/d at $r/a=z/a=0$, $Re=1.52 \times 10^4$, and two values of e . In this case, unlike the sinusoidal disturbances (Fig. 4) or type 1 random disturbances (Fig. 5), a significant increase in I_x (up to about 23%) is obtained. The Y extent where the effect of system V is felt is also greater in this case. This effect is felt at $Y/d < 0.1$. As e increases, the value of λ increases in the region $Y/d < 0.02$. Figure 7 is similar to Fig. 6, showing that as Re is increased, λ is lowered.

Figures 8 and 9 present profiles of λ with feedback system VI (employing only W2). In this case I_x actually decreases (λ is negative). This decrease becomes more pronounced as: 1) e

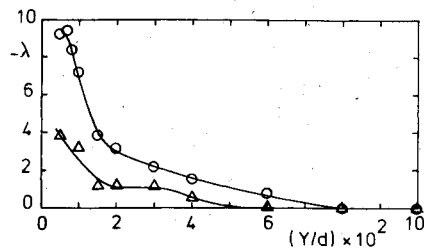


Fig. 9 Profiles of λ at $r/a=0$ with feedback system VI ($e = 3 \times 10^{-4}$ V, W1 removed, W2 at $r/a=z/a=0$). (\circ — $Re = 1.52 \times 10^4$, Δ — $Re = 6.16 \times 10^4$.)

increases (Fig. 8), $Y/d < 0.04$; and 2) Re decreases (Fig. 9). A decrease in I_x of up to about 9% has been obtained at $Y/d = 0.005$ (Fig. 8).

Feedback systems V and VI were found to be stable with e being possible to control at the required value. The reason for this is that, in practice, the disturbance injected into the flow is time delayed with respect to the $u(t)$ fluctuations sensed by W2. This time delay is expected to vary with the position of W2.

However, measurements of the nondisturbed autocorrelation function of the $u(t)$ fluctuation carried out by Alshamani¹⁵ in the fully developed region of the same channel at $y/d=0.118$ ($y=3$ mm) and $Re=1.52 \times 10^4$ indicated that this correlation function decreases from a value of 1 at a time delay of 0 to a value of about 0 at a time delay of 5×10^{-3} s. Thus the u fluctuation is correlated with itself for a time delay of less than 5×10^{-3} s. The separation between the diaphragm and W2 in the present study was about 0.13–2.54 mm. This separation gives a time delay between the diaphragm output and W2 of less than 5×10^{-3} s. Accordingly, it is reasonable to assume that a level of correlation between the disturbance (the diaphragm output) and the $u(t)$ fluctuation sensed by W2 is still maintained (in the absence of any distortion to the signal by the vib-dia system). No correlation measurements between the diaphragm output and the $u(t)$ fluctuation at W2 were, in fact, conducted. As a result, this level of correlation cannot be estimated from present measurements. However, the different effects produced by feedback systems V and VI lend support to the assumption that the disturbances RD2 are, to some extent, correlated with the $u(t)$ fluctuations at W2.

In order to give a proper interpretation of the different effects produced by the different feed systems discussed above, flow visualization experiments near the wall need to be conducted with and without the disturbances. Such studies are expected to shed more light on the effect of these disturbances on the bursting process.

It should be pointed out that this work involves turbulence measurements close to the wall, where many factors influence the hot-wire readings. These include the conduction to the wall and the flow distortion resulting from the presence of the probe. In general, the wall influence depends on the distance between the hot wire and the wall, the overheat ratio, the flow velocity, and probe geometry. Singh and Shaw¹⁶ found that the thermal conductivity of the wall material had insignificant effect. They suggested that the geometry of the needles in relation to shear flow was the primary factor causing the error. Van Thinh¹⁷ and Majola¹⁸ recommended that the hot-wire support should be maintained parallel to the direction of the mean flow. In general, there is no simple and reliable empirical or theoretical correlation that may be used for correcting the various errors in the measurements near the wall. The wall influence is best estimated on an individual basis for any given flow configuration and probe geometry. However, the work of Oka and Kostic¹⁹ and Hebbard²⁰ on the correction for wall proximity effect indicated that:

1) The noncorrected velocity profiles (plotted as U^+ vs y^+) in the viscous sublayer were universal.

2) The wall influence was negligible beyond about $y^+ = 5$.

It appears from the above discussion that data pertaining to the region $y^+ < 5$ are expected to involve errors. In the present study, no corrections were made to the data in the region $3.8 \leq y^+ \leq 5$. However, turbulence intensity measurements in this region were found to be in reasonable agreement with the equation

$$\bar{u}/U_\tau = 0.4y^+$$

given by Clark¹⁴ for the viscous sublayer region.

Summary and Conclusions

Acoustic disturbances have been injected into the fully developed region of channel flow by means of a diaphragm mounted flush with the channel wall and the effects of such disturbances on the axial turbulence intensity I_x is studied. The following conclusions may be made:

1) The application of sinusoidal acoustic disturbances, having frequencies corresponding to the inner layer bursting frequency, does not lead to a significant increase in I_x near the wall. It is, therefore, considered unlikely that the inner layer bursting phenomenon is excited by these sinusoidal disturbances.

2) The application of random acoustic disturbances (type RD1) is found to produce a small increase in I_x . At $y/d = 0.005$, the increase in I_x is about 4.5% at $Re = 1.52 \times 10^4$. This increase in I_x decreases gradually with increasing Y/d until it becomes zero at $Y/d \geq 0.02$. Inverting the sign of the disturbance has no effect on the values of I_x . It is thought unlikely that the observed increase in I_x is due to the excitation of the inner layer bursts.

3) The introduction of random disturbances (type RD2) into the region near the wall can lead to either an increase or a decrease in I_x , depending on the sign of the disturbances. For $\{\text{amp}[-u(t)]_p\}_{RD2}$, an increase in I_x of up to about 23% has been obtained at $Y/d = 0.005$. This percentage increase in I_x decreases in value with Y/d , becoming zero at $Y/d = 0.1$.

On the other hand, feeding the disturbances $\{\text{amp}[u(t)]_p\}_{RD2}$ results in a decrease in I_x . Reduction of about 9% has been obtained at $Y/d = 0.005$. The effect of the random disturbance (type RD2) at any given flow point in the neighborhood of the diaphragm becomes more pronounced with the increase in the power level of the disturbance and with the decrease of the Reynolds number.

It is suggested that the effects of the time delay and correlation between W2 and the diaphragm output should be examined in more detail in future work. In addition, it is suggested to extend the present work to study the effects of the disturbance on other turbulence quantities such as the normal component of turbulence intensity, spectra turbulence shear stress, etc.

Acknowledgments

The authors wish to thank the Department of Aeronautical and Mechanical Engineering, University of Salford, England, where this work was partially carried out. Thanks are also due to Dr. H. M. A. Samaraee, Chairman, Mechanical Engineering Department, University of Technology, Baghdad for his encouragement in the completion of the work.

References

- ¹Kline, S. J., Reynolds, W. C., Shraub, F. A., and Runstadler, P. W., "The Structure of Turbulent Boundary Layers," *Journal of Fluid Mechanics*, Vol. 30, Pt. 4, 1967, pp. 741-773.
- ²Kim, H. T., Kline, S. J., and Reynolds, W. C., "An Experimental Study of Turbulence Production near a Smooth Wall in a Turbulent Boundary Layer with Zero Pressure Gradient," Thermo-Sciences Div., Dept. of Mechanical Engineering, Stanford University, Stanford, Calif., Rept. MD-20, 1968.
- ³Corino, E. R. and Brodkey, R. S., "A Visual Investigation of the Wall Region in Turbulent Flow," *Journal of Fluid Mechanics*, Vol. 37, Pt. 1, 1969, pp. 1-30.
- ⁴Achia, B. U. and Thompson, D. W., "Structure of the Turbulent Boundary in Drag Reducing Pipe Flow," *Journal of Fluid Mechanics*, Vol. 81, Pt. 3, 1977, pp. 439-464.
- ⁵Einstein, H. A. and Li, H., "The Viscous Sublayer along a Smooth Boundary," *Proceedings ASCE, Journal of Engineering Mechanics Division*, Vol. 82, EM2, 1956, pp. 1-27.
- ⁶Morrison, W. R. B., "The Structure of Turbulence in Fully Developed Pipe Flow," Research Rept. 3/67, Dept. of Mechanical Engineering, University of Queensland, Australia, 1967.
- ⁷Rao, K. N., Narasimha, R., and Badri Narayanan, M. A., "The Bursting Phenomenon in a Turbulent Boundary Layer," *Journal of Fluid Mechanics*, Vol. 50, No. 285, 1971, pp. 339-352.
- ⁸Ueda, H. and Hinze, J. O., "Fine Structure Turbulence in the Wall Region of a Turbulent Boundary Layer," *Journal of Fluid Mechanics*, Vol. 67, Pt. 1, 1975, pp. 125-143.
- ⁹Meek, R. L., "Mean Period of Fluctuations near the Wall in Turbulent Flows," *AIChE Journal*, Vol. 18, April 1972, pp. 854-855.
- ¹⁰Blackwelder, R. F. and Kaplan, R. F., "On the Wall Structure of the Turbulent Boundary Layer," *Journal of Fluid Mechanics*, Vol. 76, Pt. 1, 1976, pp. 89-112.
- ¹¹Einstein, H. A. and Li, H., "Shear Transmission from a Turbulent Flow to Its Viscous Boundary Sublayer," Paper XIII, Heat Transfer and Fluid Mechanics Institute, University of California, 1955, pp. 1-15.
- ¹²Black, T. J., "Some Practical Applications of a New Theory of Wall Turbulence," *Proceedings of 1966 Heat Transfer and Fluid Mechanics Institute*, edited by M. A. Saad and J. A. Miller, Stanford University Press, Stanford, Calif., 1966, pp. 366-386.
- ¹³Alshamani, K. M. M., "A Study of Turbulence and Its Generation in Channel Flow," Ph.D. Thesis, University of Salford, England, 1972.
- ¹⁴Clark, J. A., "A Study of Incompressible Turbulent Boundary Layers in Channel Flows," *Transactions of ASME, Journal of Basic Engineering*, Vol. 90, Dec. 1968, pp. 455-468.
- ¹⁵Alshamani, K. M. M., "A Study of Turbulent Flow in Ducts," *Journal of Chemical Engineering*, Vol. 20, No. 1, June 1980, pp. 7-19.
- ¹⁶Singh, U. K. and Shaw, R., "Hot Wire Anemometer Measurements in Turbulent Flow Close to a Wall," *Proceedings of the DISA Conference*, The University of Leicester, edited by D. J. Cockrell, Vol. 1, Leicester University Press, England, April 1972, pp. 35-38.
- ¹⁷Van Thinh, N., "On Some Measurements Made by Means of a Hot Wire in a Turbulent Flow near a Wall," DISA Information No. 7, Jan. 1969, pp. 13-18.
- ¹⁸Majola, O. O., "The Effect of Orientation of Hot Wire Probe Body in Turbulent Shear Flow," DISA Information No. 23, 1978, pp. 24-27.
- ¹⁹Oka, S. and Kostic, Z., "Influence of Wall Proximity on Hot Wire Velocity Measurements," DISA Information No. 13, May 1972, pp. 29-33.
- ²⁰Hebbbar, K. S., "Wall Proximity Corrections for Hot Wire Readings in Turbulent Flows," DISA Information No. 25, Feb. 1980, pp. 15-16.